

---

## GENERATION OF CARBON NANOMATERIALS BY PLASMA OF A SECONDARY DISCHARGE

IU.P. VEREMII, V.YA. CHERNYAK, S.A. FILATOV<sup>1</sup>, E.M. SHPILEVSKIJ<sup>1</sup>,  
V.A. ZRAZHEVSKIJ, E.K. SAFONOV

UDC 541.16, 533.9

©2008

Taras Shevchenko Kyiv National University, Faculty of Radiophysics

(2/5, Academician Glushkov Ave., Kyiv 03022, Ukraine;

e-mail: tin@univ.kiev.ua, chern@univ.kiev.ua),

<sup>1</sup>A.V. Lykov Heat and Mass Transfer Institute of NAS of Belarus

(15, P. Brovka Str., Minsk 220072, Byelorussia)

---

We describe a plasma setup on the basis of a secondary discharge aimed at the generation of carbon nanoparticles from ethanol. The studies of the influence of modes of the processing of a raw material on the composition of final products are performed. The diagnostics was carried out by the methods of Raman scattering (RS) spectroscopy, thermogravimetric analysis (TGA), and scanning electron microscopy (SEM). The possibility to create carbon nanomaterials with different morphologies in similar systems is demonstrated.

---

### 1. Introduction

Nowadays, carbon nanodimensional structures arouse a significant interest. Surface carbon nanostructures [fullerenes and nanotubes (NTs)], like diamond, are a metastable state of condensed carbon. Therefore, the mentioned structures can be obtained only under conditions of a deviation from the thermodynamic equilibrium. Such conditions are realized, in particular, in the nonequilibrium low-temperature plasma which appears on the ignition of an arc discharge with graphite electrodes [1] and on the laser-induced ablation of graphite [2].

To obtain nanotubes, one uses, in addition to arc discharges, the processes of thermal spraying of graphite in the atmosphere of an inert gas [3]. One more efficient approach to the synthesis of carbon nanotubes (CNTs) uses the processes running on the high-temperature interaction of hydrocarbons with metallic catalysts such as the processes of thermocatalytic decay of hydrocarbons [4], chemical vapor deposition from the plasma which contains hydrocarbons [5], etc. The mentioned approaches underlie the most spread methods of synthesis of carbon nanostructures. Each of them has the intrinsic advantages and drawbacks; therefore, the researchers continue to develop new methods including some combinations of the above-mentioned ones.

The transformation of mixtures of hydrocarbons and compounds of transition metals in the plasma jet of an inert gas at the atmospheric pressure is a promising method to obtain carbon nanomaterials (CNM) which is advantageously distinguished by simplicity of its realization and the possibility of scaling among other methods of synthesis.

The use of alcohols as a source of carbon for the processes of synthesis of nanomaterials becomes traditional in a number of methods of generation. In particular, ethanol is the simplest, nonexpensive, and ecologically safe hydrocarbon which is convenient from the viewpoint of transport and efficiency on the industrial scale. In addition to ensuring the process of formation of CNM by atoms of carbon, the decaying molecules of alcohol create radicals that can further participate in the reactions of etching. Radicals and fragments which are formed on the decay of ethanol and contain oxygen can react with amorphous carbon deposited on the surface of CNM and particles of a catalyst and thus purify them [6].

In the present work, we show the results of studies of the generation of carbon nanomaterials by the plasma of a secondary discharge with the use of the vapor of ethyl alcohol (with the admixture of a catalyst) as a source of carbon. The produced CNM are studied with the help of RS-spectroscopy of light, TGA, and SEM.

### 2. Experiment

**S e t u p.** The transformation of alcohol for the processes of generation of carbon nanoparticles was executed in a plasmochemical reactor on the base of a secondary discharge with the continuous supply of the working liquid vapor to the reactor volume (Fig. 1, *a*).

The reactor was composed from metallic cylinder *1* closed by flange *3* from above. The flow of argon (the flow velocity was 3 l/min) through nozzle *4* blew off

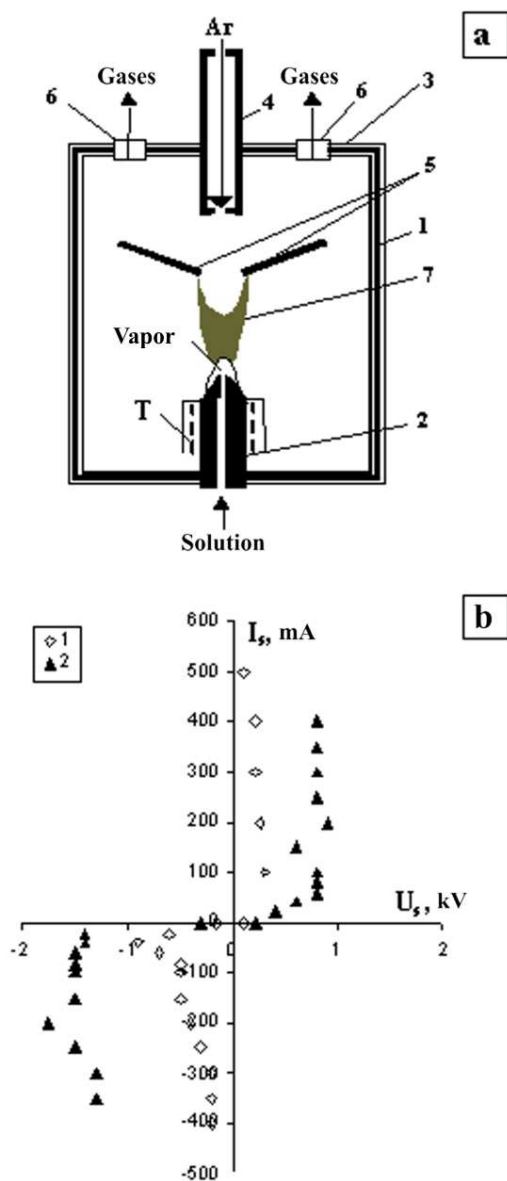


Fig. 1. Experimental setup (a) and the current-voltage characteristic of a secondary discharge (b)

the plasma of the electric arc of an auxiliary discharge 7 which burnt between two copper electrodes 5. Worked-out gases were taken out from the reactor through the exhaust system 6. The working mixture was supplied to evaporator *T* and entered into the system in the form of vapor through the 1.5-mm axial channel in the electrode of secondary discharge 2. As the second electrode of the secondary discharge, the plasma of the auxiliary discharge served. The current of the secondary discharge passed across the plasma of transverse arc discharge 7 and the working liquid vapor.

The feeding of the auxiliary and secondary discharges was performed with the help of dc sources. The polarity of the secondary discharge was determined by the sign of the electrode potential 2.

The current-voltage characteristic of the secondary discharge, which was obtained in the system without vapors of alcohol at the auxiliary discharge current  $I_d = 400$  mA, is given in Fig. 1,b (curve 1). The analysis of its form allows us to refer the secondary discharge to the transient region between glow and arc discharges. At currents  $I_s$  which exceed 300 mA, a nonself-maintained secondary discharge passes into a self-maintained one, i.e. it can burn without support by the auxiliary discharge.

After the filling of the reactor with vapors of alcohol, which occurs approximately in one minute after the supply of a working liquid into the discharge zone, the sharp change of the voltage drop on the secondary discharge happens. It increases from hundreds of Volts to 1-3 kV, and then the voltage stabilizes on the attained level. The current-voltage characteristic of the secondary discharge for the same mode of the auxiliary discharge is given by curve 2 in Fig. 1,b. We also see the qualitative change of the characteristic of the secondary discharge after the supply of alcohol: the voltage drop on the discharge does not vary practically with increase in the current. The secondary discharge does not pass into a self-maintained one, as it occurs if the vapor of alcohol is absent in the system at  $I_s \geq 300$  mA.

We introduced the solution of ethanol with the 0.004-% admixture of a catalyst (iron acetate  $\text{Fe}(\text{CH}_3\text{COO})_2$ ). The supply rate of the solution into the discharge zone was equal to 1 ml/min. The parameters of the auxiliary discharge were held on the level  $I_d=400$  mA, and  $U_d = 1 \div 1.2$  kV; those of the secondary discharge were  $I_s = 200$  mA, and  $U_s = 600 \div 800$  V. The processing duration was 1-2 h, the power of discharges was  $\sim 600$  W. During the processing, 100-200 mg of a carbon material were created. The temperature in the zone of formation of a carbon material was not controlled, and the system operated without cooling.

**Generation medium.** The mass of created carbon materials depends significantly on the temperature in the reactor and the composition of a gas mixture.

To determine the chemical composition of the gas medium, where CNM where generated, we performed the optical studies of the plasma of the secondary discharge which burnt in the vapor of alcohol. The emission spectra were registered with an optical device SL-40 at a distance of 0.5 cm from the output cut of metal electrode 2 of the

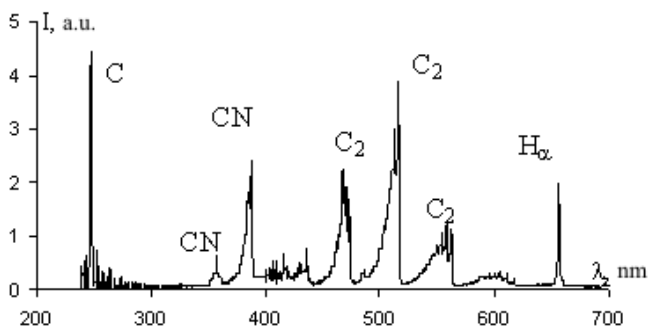


Fig. 2. Emission spectrum of plasma in the vapor of alcohol

secondary discharge. The typical emission spectrum is presented in Fig. 2, where we observe the intense bands of molecules of carbon  $C_2$  clearly represented by the Swan band system.

These bands are most intense and compose the main part of the emission, by coloring the plasma to green. The spectrum contains bands of CN (the source of nitrogen is technical argon which is the plasma-forming gas of the auxiliary discharge) represented by the violet band system lines, as well as the lines corresponding to atoms of carbon C (247.8 nm) and hydrogen  $H_\alpha$  (656 nm) [7].

It is worth noting the considerable content of hydrogen atoms in the discharge zone. It is well known that an increase in the amount of hydrogen in the gas phase promotes a decrease of amorphous pyrocarbon and causes the increase in the share of products possessing a more organized structure [8]. The enhancement of the temperature of the process also promotes the formation of CNM with a more graphitized structure. But, as the temperature grows, the supply rate of carbon from the gas phase to metallic particles of the catalyst begins to exceed the rate of diffusion of atoms of carbon, which leads to the carbonizing of catalytic particles and the termination of the growth of nanotubes and nanofibers [8].

Method of post-processing of the obtained carbon black. The produced carbon powder was mechanically collected from all internal elements of the reactor, mixed, and weighed. Then CNM was subjected to the physico-chemical procedure of purification. First, a powder was treated by concentrated hydrochloric acid for a half-hour to remove the metal of a catalyst, then was washed out many times with distillate, and was dried at 100 °C. Further, the specimens were annealed in a muffle furnace with the access of air at various temperatures

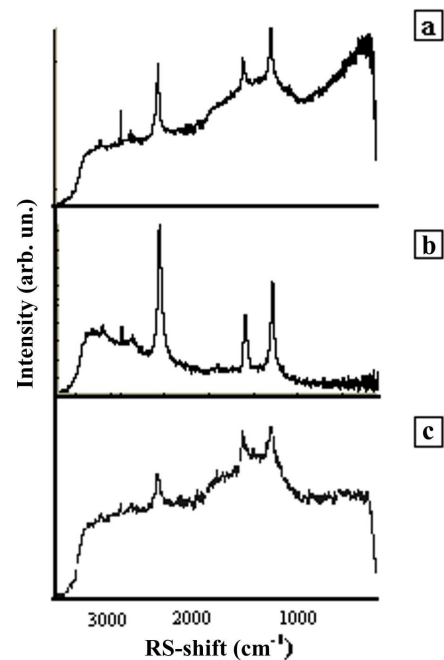


Fig. 3. RS-spectra of specimens which contain *a* – nanotubes, *b* – nanofibers, and *c* – nanodiamonds

(300–500 °C, 0.5 h) in order to oxidize amorphous carbon and particles with weakly graphitized structure.

### 3. Results of the Diagnostics

R S. The method of RS-spectroscopy of light is most perspective and gives the greatest amount of information as compared with the other available methods of optical diagnostics of nanotubes. This method allows one to reliably determine the content of CNT or other allotropic forms of carbon in a specimen. The excitation of RS-spectra in the IR-region allows us to analyze the specimens in the presence of amorphous carbon.

To realize the Raman scattering of light, we used a laser with a wavelength of 1064 nm.

The RS-spectra of specimens allow us to determine the presence of their fractions with different morphologies (Fig. 3). For example, the presence of radial breathing modes (RBM) in the spectra of some specimens indicates the presence of carbon nanotubes (Fig. 3,*a*). The ratio of the tangential modes of the spectra of other specimens is characteristic of carbon nanofibers (NFs) of the cone type (Fig. 3,*b*). In the RS-spectra of specimens of the third group, we observe the presence of bonds C–C characteristic of diamond ( $sp^3$ -hybridization). They correspond to carbon

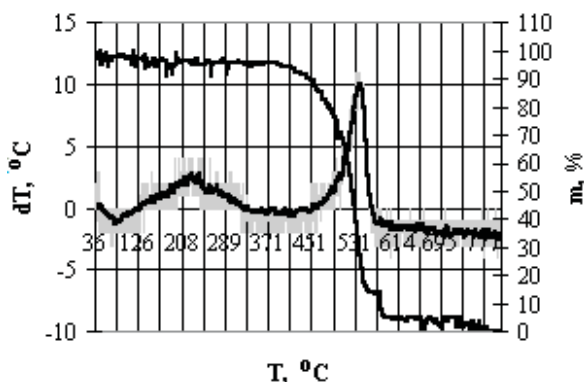


Fig. 4. Result of TGA

nanostructures which are based on the graphite lattice – the so-called diamond-like carbon nanostructures – nanodiamonds (NDs, Fig. 3,c). All these data well correlate with the results obtained by SEM.

It is important to note that, all specimens obtained on the realization of the secondary discharge with positive polarity are characterized by the presence of diamond-like carbon nanostructures. The yield of the final product also strongly depends on the means of post-processing of the produced CNM, and physical and chemical characteristics of a method. After the purification of specimens (the annealing was realized at a temperature of 300 °C), we observe the appearance of RBM in the RS-spectra, which indicates the presence of NTs.

With increase in the temperature of oxidation, we observe, in the first turn, the burn-off of graphite and, respectively, the increase of a share of CNT in a specimen, which is confirmed by the appearance and intensification of the breathing mode. The formation of CNT is also possible directly in the process of destruction of graphite, because the initial spectra contain no traces of NTs. The presence of CNT in specimens after the oxidation can be also indicated by the fact that the  $G'$ -mode intensity becomes lower than those of the  $D$ - and  $G$ -modes. A decrease in the  $G'$ -mode intensity testifies to the breaking of bonds between graphene sheets, which can correspond to the destruction of formed carbon nanofibers, rather than directly of graphite.

T G A. In Fig. 4, we present the result of TGA of a specimen with CNM. This method consists in the control over the weight of a specimen on its heating with a certain rate (in our case, 6 °C/min) in a chamber with the access of air. The burn-off of amorphous carbon begins from 380 °C [11], and the smooth curve with shoulders at 470 and 570 °C is related to the presence of

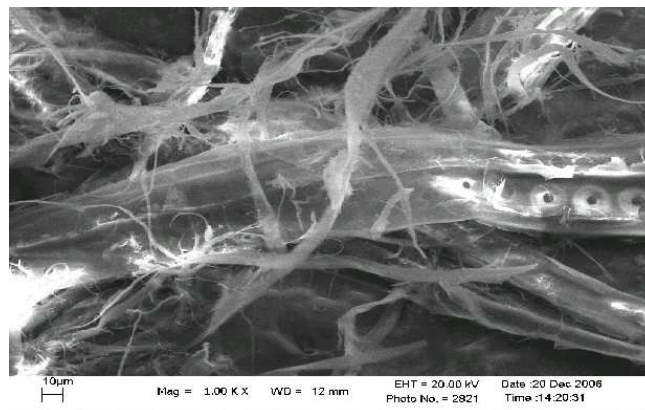


Fig. 5. Photo of a specimen containing NTs and NFs

different phases in the specimen. One of the version of the formation of shoulders can be related to the process of burning of one of the phases of a specimen, which is accompanied by the process of sublimation of another phase, for which, respectively, the additional thermal energy is needed. In the case where the energy released on the burning is close to the energy which consumed on the sublimation, a change in the mass of a specimen can happen without remarkable change in its temperature. In survey [9], the presence of shoulders on the curves of thermogravimetric data is ascribed to the maximum of the rate of oxidation of various fractions of CNM, in particular, of one-layer carbon nanotubes (471 °C) and fullerene molecules (568 °C).

S E M. In the photo of a specimen obtained on the realization of the mode with  $I_s = 400$  mA,  $U_s = 600$  V;  $I_d = 400$  mA,  $U_d = 1.4$  kV with negative polarity of the secondary discharge, we see the sprouts of NTs and NFs with different structures and diameters (Fig. 5). The considerable contribution to the RS-spectra of this specimen was also made by nanofibers.

In the general photo of a specimen obtained on the realization of the mode with  $I_s = 400$  mA,  $U_s = 200$  V;  $I_d = 200$  mA,  $U_d = 400 \div 500$  V with positive polarity of the secondary discharge (Fig. 6,a), we see microplates and strips (possibly, the sprouts or bundles of NTs). At high magnifications, the microplates demonstrate various nanostructures: one of them (Fig. 6,b) shows the presence of nanodiamonds, and the plate on the right includes fractal formations (Fig. 6,c). The RS-spectrum of the given specimen indicates the presence of diamond-like carbon nanostructures.

Of certain interest are the fractal formations of the spherical form with the characteristic size of about one micron (Fig. 6,c). In view of the latest studies of the

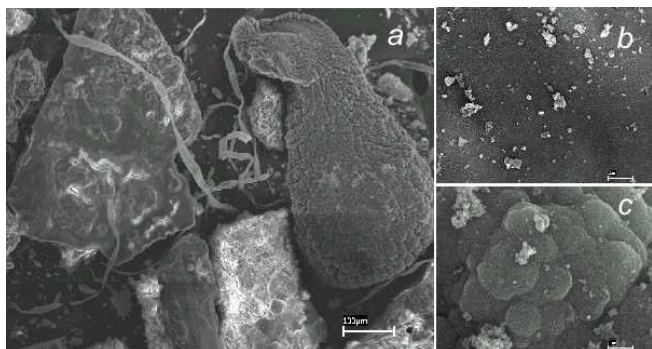


Fig. 6. Photo of a specimen containing NDs

nature of nanodiamonds, we can refer these formations to a new intermediate phase of carbon. It was established that, as the size of a nanodiamond decreases, its structure becomes unstable. The quantum-mechanical modeling showed the graphitization of the first atomic layer which is accompanied by the formation of pentagonal connections of fragments of graphene with atoms positioned below. This ensures the further bending of the surface which acquires, in the course of time, the geometry similar to a half of fullerene [10]. It was established in experiments that the majority of nanodiamonds has size of about 4 nm, and their surface is covered by a mixture of atoms of carbon with  $sp^2$ - and  $sp^3$ -bonds [11]. Thus, it was shown that a nanodimensional diamond has, indeed, diamond base with a fullerene-like reconstruction of the surface. Such carbon particles are named “bucky diamonds”. The results of modeling of the relative stability of various allotropic structures of carbon showed that “bucky diamonds” occupy the domain of existence which covers the calculated upper bound of stability of a fullerene and the lower bound of stability of a nanodiamond [12].

#### 4. Conclusions

The significant correlation between the results of RS-spectroscopy, TGA, and SEM indicates the possibility to obtain nanofibers, nanotubes, fullerenes, and nanodiamonds in the given plasma system.

Depending on the mode of operation of the system, we can generate nanostructures with different morphologies. If the negative polarity of the secondary

discharge is realized, then NTs and NFs are mainly formed. On the positive polarity of the secondary discharge, NDs are created.

It is possible that some components of CNM are formed not only in the process of intermediate operation of the plasma system, but also during the post-processing.

This work is carried out under the support by grant N 06BP05203 of Taras Shevchenko Kyiv National University.

1. W. Kratshmer, *Nature* **347**, 354 (1990).
2. H.W. Kroto *et al.*, *Nature* **318**, 162 (1985).
3. T. Guo *et al.*, *Chem. Phys. Lett.* **243**, 49 (1995).
4. M.J. Yacaman *et al.*, *Appl. Phys. Lett.* **62**, 202 (1993).
5. C. Bower *et al.*, *Appl. Phys. Lett.* **77**, 2767 (2000).
6. A.G. Nasibulin *et al.*, *J. of Nanopart. Research.* **8**, 456 (2006).
7. A.G. Gaydon, *The Spectroscopy of Flames* (Chapman and Hall, London, 1957).
8. A.A. Volodin *et al.*, in *Proceedings of III International Sympos.* (Minsk, 2004), p.116.
9. A.V. Eletsky, in *Encyclopedia of Low-Temperature Plasma* (Yanus-K, Moscow, 2006) Vol. XI-5, p. 223 (in Russian).
10. J.-Y. Raty, G. Galli, C. Bostedt *et al.*, *Phys. Rev. Lett.* **90**, 037401 (2003).
11. A.E. Aleksenskii, M.V. Baidakova, A.Ya. Vul', and V.I. Siklitskii, *Physics of Solid State* **41**, 668 (1999).
12. A.S. Barnard, S.P. Russo *et al.*, *Phys. Rev. B* **68**, 073406 (2003).

Translated from Ukrainian by V.V. Kukhtin

#### УТВОРЕННЯ ВУГЛЕЦЕВИХ НАНОМАТЕРІАЛІВ В ПЛАЗМІ ВТОРИННОГО РОЗРЯДУ

Ю.П. Веремій, В.Я. Черняк, С.А. Філатов,  
Е.М. Штмлевський, В.А. Зражевський, Є.К. Сафонов

#### Резюме

Описано плазмову установку на базі вторинного розряду для генерації вуглецевих наночастинок з етанолу. Проведено дослідження впливу режимів обробки сировини на склад кінцевих продуктів. Для діагностики були використані методи спектроскопії комбінаційного розсіяння світла (КРС), термогравіметричного аналізу (ТГА) і растрової скануючої мікроскопії (РСМ). Показано можливість генерації в подібних системах вуглецевих наноматеріалів різної морфології.